Precise spectroscopy of antiprotonic helium and sensitivity of transitions to the antiproton mass

V.I. Korobov

Joint Institute for Nuclear Research

141980, Dubna, Russia

This contribution is devoted to precise numerical calculation of transition intervals between metastable states in the antiprotonic helium atom. The final uncertainty is estimated to be about 1–2 MHz, which complies with requirements of recent measurements of the ASACUSA group at CERN.

1 Introduction

Some time ago a fraction of metastable states of antiprotons in helium had been discovered [1]. Later [2, 3] using laser spectroscopy a model explaining this metastability had been unambiguously established based on Condo's hypothesis [4], which suggests the existence of long-lived states in a new exotic three-body system — antiprotonic helium atoms. Since this pioneering work experimental precision has been improved by more than three orders of magnitude [5] and does require precise theoretical consideration.

The study of the antiprotonic helium metastable states has a manifold interest.

First and the most obvious is its exotic nature. Antiprotons as antimatter survive in helium media within the time scale which is about 6(!) orders of magnitude larger than generally for antiprotons in matter. As atomic system it is of no less surprise, since the metastable states are imbedded into the continuum and still are more stable than usual excited bound states in atoms. In that sense this example of metastability deserves to be included into textbooks on the nonrelativistic quantum mechanics along with an example of Efimov's states [6].

Other motivation can be found in metrology of fundamental constants. As it was already mentioned the experimental precision has been increased during the last few years by 3 orders of magnitude and further improvement is foreseen [5]. It means that an antiproton mass from these experiments can be extracted with a higher precision than

now available for a proton. A study of the hyperfine structure can bring us valuable information on antiproton magnetic moment and electromagnetic finite size structure.

It is known that quantum electrodynamics is well developed for the two–body bound systems [12]. On the other hand, the major part of the proposed methods, such as the Bethe-Salpeter equation or the effective Dirac equation, do not extend well on systems of three and more particles. So, the problem of three–body QED bound states is of great importance for better understanding of QED. For theory it is extremely essential to have as much of precise experimental data as possible. Unfortunately, the three-body precise spectroscopy is basically limited by the helium atom, where the external field approximation for a system of two electrons can be used. Below are some examples that are presently available:

1. Helium atom fine structure of 2^3P_J-state:

$$\nu_{\rm exp}(2^3P_1-2^3P_0) \quad = 29\,616\,950.9 \pm 0.9 \text{ kHz}, \quad [7]$$
$$\nu_{\rm theory}(2^3P_1-2^3P_0) = 29\,616\,944 \pm 10 \text{ kHz}, \quad [8]$$

2. Ionization potential of the ground state of helium:

$$\nu_{\rm exp}(1^1S) \quad = 5\,945\,204\,238 \pm 45 \text{ MHz}, \quad [9]$$
$$\nu_{\rm theory}(1^1S) = 5\,945\,204\,223 \pm 42 \text{ MHz}, \quad [10]$$

3. Antiprotonic helium transition intervals:

$$\nu_{\rm exp}[(39,35) \to (38,34)] \quad = 501\,948\,800 \pm 40 \text{ MHz}, \quad [11]$$
$$\nu_{\rm theory}[(39,35) \to (38,34)] = 501\,948\,755.6 \pm 1.3 \text{ MHz}, \quad [\text{this talk}]$$

Accuracy of modern experimental data for positive molecular ions of hydrogen isotopes (H_2^+, HD^+, etc) is much below the theoretical uncertainty, which can be achieved using the present level of the QED bound state theory for such systems. Recently, two experimental groups announced a program of the two photon spectroscopy of the hydrogen molecular ions [13, 14].

In this work relativistic and radiative corrections for the Coulomb three body problem are derived from a formalism of the nonrelativistic quantum electrodynamics (as it was formulated in [15]). This formalism seems to be the most suitable for extending the theory of bound states in QED to systems with a number of particles greater than two. An energy of a bound state is searched as a series expansion in terms of the coupling constant α. Solution is obtained up to and including terms of the $\alpha^5 \ln^2 \alpha \cdot \mathrm{Ryd}$ order.

2 Numerical study of the nonrelativistic Hamiltonian for the antiprotonic helium atom

Numerical calculation of the nonrelativistic energies is one of the challenging problems in theoretical studying of the antiprotonic helium atoms. The three main features are

essential for numerical treatment of the metastable states are: high total angular momentum $L \sim 34$, location of the states in a continuum spectrum (resonances), and the adiabaticity.

The two approaches were applied to calculate these states.

The first one is the Feshbach formalism, and is an attempt to circumvent the difficulties connected with the resonant nature of the metastable states and especially useful for the states with small Auger decay rate, much smaller than the radiative decay rate. In the Feshbach formalism, the identity operator for the Hilbert space of states of the system is split onto a sum of two projection operators,

$$I = P + Q, \tag{1}$$

where P and Q are orthogonal and operator P projects on the subspace of closed channels. Then the Schrödinger equation:

$$(H - E)\Psi = 0, \quad H = \begin{pmatrix} H_{PP} & H_{PQ} \\ H_{QP} & H_{QQ} \end{pmatrix}, \tag{2}$$

can be formally reduced to the subspace of closed channels as follows:

$$\left\{(H_{PP} - E) + \left[H_{PQ}(E - H_{QQ})^{-1}H_{QP}\right]\right\}\Psi_P = 0. \tag{3}$$

An operator in square brackets is called "optical potential", which is a complex valued, energy dependent function.

Molecular expansion for the wave function [16] is particularly useful since already the simple adiabatic Born-Oppenheimer approach provides reasonably accurate closed channel solution. For the state with total orbital angular momentum L, total spatial parity λ this expansion has a form:

$$\Psi_M^{L\lambda}(\mathbf{R}, \mathbf{r}) = \sum_{m=0}^{L} \mathcal{D}_{Mm}^{L\lambda}(\Phi, \Theta, \varphi) F_m^{L\lambda}(R, r, \theta), \tag{4}$$

where amplitude $F_m^{L\lambda}(R, r, \theta)$ falls down with azimuthal quantum number m as $\sim (m_e/M_{\bar{p}})^m$. If one retains in the expansion only the components with azimuthal number m less than the minimal multipolarity [17] of the Auger transition from this state, one gets a projection onto the subspace of closed channels. And thus the standard variational procedure can be applied in order to get an approximate solution. If the minimal multipolarity Δl is a number greater than 4, then the variational solution may be obtained with accuracy sufficient for precise spectroscopy of the antiprotonic helium atoms.

In what follows we assume that the "optical potential" is omitted and only a solution for a subspace of closed channels is obtained as a zero order approximation, which is then used for higher order relativistic and radiative corrections.

The present day experiments are usually carried out for the transitions, in which the daughter state has a short Auger life-time, in order to observe a spike in the Antiproton Annihilation Time Spectrum. In this case the resonance nature is important for

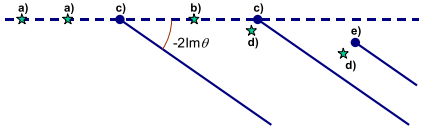

a) Discrete eigenvalues of H
b) Continuum embedded eigenvaues
c) Thresholds
d) Resonance eigenvalues
e) Complex thresholds

Figure 1: Spectrum of $H(\theta)$.

the numerical treatment of these states and we use the Complex Coordinate rotation (CCR) method for getting the nonrelativistic energies and the leading order relativistic corrections from the Breit–Pauli Hamiltonian.

The basics of the CCR method are briefly expounded below (for a detailed review see [18]). The Coulomb Hamiltonian is analytic under dilatation transformations

$$(U(\theta)f)(\mathbf{r}) = e^{m\theta/2} f(e^{\theta}\mathbf{r}), \tag{5}$$

for real θ and can be analytically continued to the complex plane.

The CCR method "rotates" the coordinates of the dynamical system

$$r_{ij} \to r_{ij}e^{i\varphi}, \qquad \theta = i\varphi$$

where φ is the parameter of the complex rotation.

Under this transformation the Hamiltonian changes as a function of φ

$$H_{\varphi} = Te^{-2i\varphi} + Ve^{-i\varphi}, \tag{6}$$

and the continuum spectrum of H_{φ} is rotated on the complex plane around branch points ("thresholds") to "uncover" resonant poles situated on the unphysical second sheet of the Reimann surface in accordance with the Augilar-Balslev-Combes theorems [19]. The structure of the spectrum of the rotated Hamiltonian is shown in Figure 1.

For numerical calculations we use the two sets of physical constants. The CODATA98 recommended values: $m_{^4\mathrm{He}} = 7294.29951\, m_e$, $m_{^3\mathrm{He}} = 5495.88524\, m_e$, $m_{\bar{p}} = 1836.152667\, m_e$, $a_e = 0.0011596522$, $a_p = 1.792847337$, $\alpha = 7.297352533 \cdot 10^{-3}$, $R_{\infty}c = 3289841960.368$ MHz, and $a_0 = 52917.7208$ fm. They are necessary for comparison

N	E_{nr}	$\Gamma/2$	$\delta(\mathbf{r}_{\mathrm{He}})$
2200	$-2.83652459643(3)$	$1.63 \cdot 10^{-9}$	1.584820
2800	$-2.83652459642(1)$	$1.61 \cdot 10^{-9}$	1.5848224
3400	$-2.836524596415(3)$	$1.606 \cdot 10^{-9}$	1.5848228

Table 1: The nonrelativistic energy, E_{nr}, half-width, $\Gamma/2$, and $\langle\delta(\mathbf{r}_{\mathrm{He}})\rangle$ of the $(38, 34)$ state of $^4\mathrm{He}^+\bar{p}$ atom as functions of basis set.

state	E_{nr}	$\Gamma/2$	$\delta(\mathbf{r}_{\mathrm{He}})$	$\Delta E_{\Delta m}$
$(31,30)$	$-3.507372719686(2)$	$3.341\cdot10^{-9}$	0.9936885	61.68 MHz
$(32,31)$	$-3.34883217260011(1)$	$5.16\cdot10^{-12}$	1.0689408	56.70 MHz
$(33,31)$	$-3.219507251133(2)$	$8.279\cdot10^{-9}$	1.1871603	51.68 MHz
$(34,32)$	$-3.0944509665400(4)$	$1.72\cdot10^{-11}$	1.2729449	47.31 MHz
$(35,32)$	$-2.995404358273(2)$	$8.162\cdot10^{-9}$	1.3951957(3)	42.94 MHz
$(35,33)$	$-2.983373123458(2)$	—	1.3630400	43.20 MHz
$(36,33)$	$-2.8971922878372(3)$	$\mathbf{2.93\cdot10^{-11}}$	1.4866059	39.11 MHz
$(37,33)$	$-2.821963030784(4)$	$4.268\cdot10^{-9}$	1.604040(1)	35.41 MHz
$(36,34)$	$-2.88491261933851(4)$	—	1.4569802	39.32 MHz
$(38,34)$	$-2.7451741489560(8)$	$3.8\cdot10^{-12}$	1.6942064	32.05 MHz

Table 2: Nonrelativistic energies (CODATA02), E_{nr}, half-widths, $\Gamma/2$, and the expectation value of $\langle\delta(\mathbf{r}_{\mathrm{He}})\rangle$ for individual states of $^3\mathrm{He}^+\bar{p}$. Last column: $\Delta E_{\Delta m} = E_{\mathrm{CODATA98}} - E_{\mathrm{CODATA02}}$.

with previous calculations [20]. The other set is the CODATA02 recommended values: $m_{^4\mathrm{He}} = 7294.299536\,m_e$, $m_{^3\mathrm{He}} = 5495.885269\,m_e$, $m_{\bar{p}} = 1836.1526726\,m_e$, $a_e = 0.001159652186$, $a_p = 1.792847351$, $\alpha = 7.297352568\cdot10^{-3}$, $R_\infty c = 3289841960.360$ MHz, and $a_0 = 52917.72108$ fm.

Convergence of the nonrelativistic energies for individual states was checked during the calculation (see Table 1). Special attention was payed to numerical convergence of mean values of the delta function operators. It is of great importance to keep control of uncertainty in delta functions, which eventually determines the uncertainty of the leading order relativistic correction.

Nonrelativistic energies for individual states in $^3\mathrm{He}^+\bar{p}$ atom are presented in Table 2. The numerical calculations were performed with the CCR method, which allows to determine along with the nonrelativistic energies precise values for nonrelativistic Auger width and the relativistic leading order corrections from the Breit–Pauli Hamiltonian. The dash line for some entries of Auger width means that for these states the Feshbach projection formalism was used and the numerical uncertainty connected with the limitations of this approach is not essential for the present level of accuracy. In a previous work [20] initial states of transitions were treated using the Feshbach formalism, because it was expected that the zero order approximation for the nonrelativistic wave function would be accurate enough with this approach. That is not really true, and is clearly seen in the case of state $(36,33)$, which is marked boldface in the Table, the Auger width for this state is more than an order of magnitude larger than the radiative width and the use of simple Feshbach formalism leads to large errors of $\sim$30 MHz.

Comparison with previous results [20] is presented in Table 3. In general the new data are within the error bounds of earlier calculations. In those cases where shift exceeds indicated uncertainty it can be attributed to more accurate CCR treatment of initial (parent) states for these transitions. The use of the simple closed channels formalism does not allow to determine accurate error bounds for theoretical values.

	2003	2005	ΔE
$(32,31) \to (31,30)$	1043128576(4)	1043128574.7(1.1)	1
$(34,32) \to (33,31)$	822809178(6)	822809166.3(1.2)	**12**
$(36,33) \to (35,32)$	646180434(5)	646180404.6(1.2)	**30**
$(36,34) \to (37,33)$	414147518(6)	414147511.7(2.2)	4
$(38,34) \to (37,33)$	505222293(5)	505222276.9(2.0)	**16**
$(32,31) \to (31,30)$	1132609218(5)	1132609219.1(1.0)	-1
$(35,34) \to (33,32)$	804633053(3)	804633054.3(1.2)	-1
$(37,34) \to (36,33)$	636878159(5)	636878148.7(1.2)	**10**
$(37,35) \to (38,34)$	412885129(6)	412885134.9(2.3)	-5
$(39,35) \to (38,34)$	501948765(5)	501948752.7(1.3)	**12**
$(40,35) \to (39,34)$	445608567(20)	445608567.2(2.0)	0

Table 3: Comparison of the old data [20] for the transition energies (in MHz) with the results of this presentation. CODATA'98 values are used for convenience of comparison. Last column shows changes of transition energy, which are primarily due to improved numerical solution.

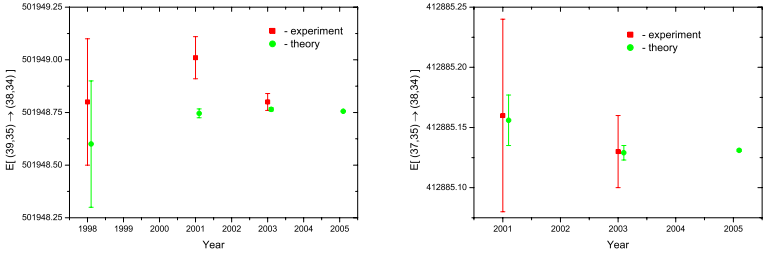

Figure 2: Improvement of theoretical and experimental precision in past years.

Figure 2 illustrates progress achieved in theoretical and experimental studies of the transition intervals for the antiprotonic helium atoms.

3 Higher order corrections

To specify explicitly relativistic and radiative corrections, which are included into calculations, we list here a set of equations for these contributions.

Relativistic correction for the bound electron:

$$E_{rc} = \alpha^2 \left\langle -\frac{\mathbf{p}_e^4}{8m_e^3} + \frac{1}{8m_e^2}\left[Z_{\rm He} 4\pi\delta(\mathbf{r}_{\rm He}) + Z_{\bar p} 4\pi\delta(\mathbf{r}_{\bar p})\right] \right\rangle . \qquad (7)$$

Radiative corrections for the bound electron (anomalous magnetic moment):

$$E_{rc-qed} = \alpha^2 \left\langle \frac{2a_e}{8m_e^2} \left[Z_{\rm He} 4\pi\delta(\mathbf{r}_{\rm He}) + Z_{\bar p} 4\pi\delta(\mathbf{r}_{\bar p}) \right] \right\rangle, \tag{8}$$

where $a_e = \frac{\alpha}{\pi}\cdot\frac{1}{2} + \left(\frac{\alpha}{\pi}\right)^2 \left[\frac{197}{144} + \frac{\pi^2}{12} - \frac{\pi^2}{2}\ln 2 + \frac{3}{4}\zeta(3)\right] = 1.1596522\cdot 10^{-3}$ is the anomalous magnetic moment of electron.

One transverse photon exchange correction of the leading order α^2:

$$E_{exch} = \alpha^2 \frac{Z_i}{2m_e m_i} \left\langle \frac{\mathbf{p}_i \mathbf{p}_e}{r_i} + \frac{\mathbf{r}_i (\mathbf{r}_i \mathbf{p}_i) \mathbf{p}_e}{r_i^3} \right\rangle. \tag{9}$$

One-loop transverse photon self-energy corrections:

$$E_{se} = \alpha^3 \frac{4Z_i}{3m_e^2} \langle \delta(\mathbf{r}_i) \rangle \left\{ \left[\ln\frac{1}{\alpha^2} - \beta + \frac{5}{6} - \frac{3}{8} \right] + (Z_i\alpha) 3\pi \left(\frac{139}{128} - \frac{1}{2}\ln 2 \right) - \frac{3}{4}(Z_i\alpha)^2 \ln^2 \frac{1}{(Z_i\alpha)^2} \right\}, \tag{10}$$

where $\beta = \ln k_0(n)/R_\infty$ is the Bethe logarithm of the three-body state.

One transverse photon exchange corrections of order α^3:

$$E_{\alpha^3-rec} = \frac{Z_i\alpha^3}{m_e m_i} \left\{ \frac{2}{3} \left(-\ln\alpha - 4\beta + \frac{31}{3} \right) \langle \delta(\mathbf{r}_i) \rangle - \frac{14}{3} \langle Q(r_i) \rangle \right\}, \tag{11}$$

where $Q(r)$ is the so-called Araki-Sucher term.

One-loop vacuum polarization:

$$E_{vp} = \frac{4Z_i\alpha^3}{3m_e^2} \left[-\frac{1}{5} + (Z_i\alpha)\pi\frac{5}{64} \right] \langle \delta(\mathbf{r}_i) \rangle. \tag{12}$$

Relativistic corrections for heavy particles:

$$E_{kin} = \alpha^2 \left\langle -\frac{\mathbf{p}_{\rm He}^4}{8m_{\rm He}^3} - \frac{\mathbf{p}_{\bar p}^4}{8m_{\bar p}^3} + \frac{(1+2a_{\bar p})Z_{\bar p}}{8m_{\bar p}^2} 4\pi\delta(\mathbf{r}_{\bar p}) \right\rangle, \tag{13}$$

Two-loop QED corrections:

$$E_{two-loop} = \alpha^4 \frac{Z_i}{m_e^2\pi} \left[-\frac{6131}{1296} - \frac{49\pi^2}{108} + 2\pi^2\ln 2 - 3\zeta(3) \right] \langle \delta(\mathbf{r}_i) \rangle. \tag{14}$$

Finite nuclear size corrections:

$$\Delta E_{\rm nuc} = \sum \frac{2\pi Z_i (R_i/a_0)^2}{3} \langle \delta(\mathbf{r}_i) \rangle, \tag{15}$$

where R is the root-mean-square radius of the nuclear charge distribution. The rms radius for isotope nuclei and antiproton is, respectively,

$$R(^4{\rm He}) = 1.673(1)\ {\rm fm}, \qquad R(^3{\rm He}) = 1.844(45)\ {\rm fm}, \qquad R(\bar p) = 0.862(12)\ {\rm fm}.$$

The α^4 relativistic correction (an accuracy of this approximate formula is about 10%)

$$E_{\alpha^4} \approx -\alpha^4 \frac{\pi}{2} \delta(\mathbf{r}_{\rm He}). \tag{16}$$

4 Hellman-Feynman theorem and dependence of transitions on physical constants

If the Hamiltonian H_0 depends on some parameter μ, the *Hellman-Feynman* theorem is fulfilled:

$$\frac{\partial E_0}{\partial \mu} = \left\langle \psi_0 \left| \frac{\partial H_0}{\partial \mu} \right| \psi_0 \right\rangle . \tag{17}$$

For the nonrelativistic Hamiltonian (in a.u.)

$$H_0 = \frac{\mathbf{p}_1^2}{2\mu_{12}} + \frac{\mathbf{p}_2^2}{2\mu_{13}} + \frac{m_e}{m_1}\mathbf{p}_1\mathbf{p}_2 + \frac{z_1 z_2}{r_{12}} + \frac{z_1 z_3}{r_{13}} + \frac{z_2 z_3}{r_{23}} , \tag{18}$$

dependence on mass ratios: $\eta_{32} = m_3/m_2$ and $\eta_{21} = m_2/m_1$ can be easily expressed:

$$\frac{1}{2\mu_{12}} = \frac{(1+\eta_{21})\eta_{32}}{2}, \qquad \frac{1}{2\mu_{13}} = \frac{1+\eta_{21}\eta_{32}}{2}, \quad \text{and} \quad \frac{m_3}{m_1} = \eta_{21}\eta_{32}.$$

Then

$$\begin{aligned} \frac{\partial E_0}{\partial \eta_{32}} &= \frac{1+\eta_{21}}{2}\left\langle \mathbf{p}_1^2 \right\rangle + \frac{\eta_{21}}{2}\left\langle \mathbf{p}_2^2 \right\rangle + \eta_{21}\left\langle \mathbf{p}_1\mathbf{p}_2 \right\rangle , \\ \frac{\partial E_0}{\partial \eta_{21}} &= \frac{\eta_{32}}{2}\left\langle \mathbf{p}_1^2 \right\rangle + \frac{\eta_{32}}{2}\left\langle \mathbf{p}_2^2 \right\rangle + \eta_{32}\left\langle \mathbf{p}_1\mathbf{p}_2 \right\rangle . \end{aligned} \tag{19}$$

It is more convenient to use a dimensionless form:

$$\Delta E_0 = \left(\eta_{32}\frac{\partial E_0}{\partial \eta_{32}}\right)\left(\frac{\Delta\eta_{32}}{\eta_{32}}\right) + \left(\eta_{21}\frac{\partial E_0}{\partial \eta_{21}}\right)\left(\frac{\Delta\eta_{21}}{\eta_{21}}\right) \tag{20}$$

Coefficients: $a_{32} = \eta_{32}(\partial E_0/\partial\eta_{32})$ and $a_{21} = \eta_{21}(\partial E_0/\partial\eta_{21})$, are called normalized sensitivities and can be easily tabulated using Eq. (19).

As an example one can consider the $(39,35)\to(38,34)$ transition in $^4\mathrm{He}^+\bar{p}$ atom and estimate an energy shift due to change from CODATA98 to CODATA02 recommended values.

$$\begin{aligned} \Delta E &= (2\,\mathrm{Ry})\left[(a_{32}^{(i)} - a_{32}^{(f)})\left(\frac{\Delta\eta_{32}}{\eta_{32}}\right) + (a_{21}^{(i)} - a_{21}^{(f)})\left(\frac{\Delta\eta_{21}}{\eta_{21}}\right)\right] \\ &= (2\,\mathrm{Ry})\left[(1.6822-1.5183)\left(\frac{\Delta\eta_{32}}{\eta_{32}}\right) + (0.3382-0.3053)\left(\frac{\Delta\eta_{21}}{\eta_{21}}\right)\right] = 2.85\ \mathrm{MHz} \end{aligned}$$

This is exactly what we get from direct numerical calculation.

Having the normalized sensitivities tabulated one can perform accurate fitting of the antiproton/electron and antiproton/nucleus mass ratios from an experimental data.

	transition	ν (in MHz)	$\Delta\nu_{\text{CODATA02}-\text{CODATA98}}$
$^4\text{He}^+\bar{p}$	$(40,35) \to (39,34)$	445 608 569.8**(2.0)**(1.2)	2.61 MHz
	$(39,35) \to (38,34)$	501 948 755.6(1.3)	2.85 MHz
	$(37,35) \to (38,34)$	412 885 131.5(2.3)	−3.42 MHz
	$(37,34) \to (36,33)$	636 878 152.0(1.3)	3.29 MHz
	$(36,34) \to (35,33)$	717 474 001.8(1.3)	3.30 MHz
	$(35,33) \to (34,32)$	804 633 058.2(1.2)	3.93 MHz
	$(32,31) \to (31,30)$	1 132 609 223.6(1.0)	4.53 MHz
$^3\text{He}^+\bar{p}$	$(38,34) \to (37,33)$	505 222 280.5**(2.0)**(1.3)	3.36 MHz
	$(36,34) \to (37,33)$	414 147 507.8(2.2)	−3.91 MHz
	$(36,33) \to (35,32)$	646 180 408.4(1.4)	3.83 MHz
	$(35,33) \to (34,32)$	730 833 929.7(1.3)	4.11 MHz
	$(34,32) \to (33,31)$	822 809 170.7(1.2)	4.37 MHz
	$(32,31) \to (31,30)$	1 043 128 579.7(1.1)	4.98 MHz

Table 4: Theoretical values of transition frequencies ν (in MHz) between metastable states, which were measured in experiment. Calculations are performed with CODATA02 recommended values. Last column shows the energy shift due to change from CODATA98 to CODATA02 values of physical constants. Marked boldface is the numerical uncertainty due to a finite variational basis set.

5 Numerical results

Results of numerical calculations are summarized in Table 4. For transitions $(40,35) \to (39,34)$ for the $^4\text{He}^+\bar{p}$ atom and $(38,34) \to (37,33)$ for the $^3\text{He}^+\bar{p}$ atom it was found that the numerical uncertainty still exceeds the theoretical one. A latter is defined by the yet uncalculated higher order contributions in expansion in the fine structure constant α. As is seen from the Table the best candidates for determination of the antiproton mass are the lowest transitions with the smallest principal quantum number n of the antiproton orbital. For these transitions theoretical uncertainty is lower and the transition frequency is larger. It is worthy to note that numerically the low n, low v states are most tractable and computational accuracy is the highest for these states.

Acknowledgements

It is a great pleasure for me to thank Eberhard Widmann and the Local Organizing Committee for this generous opportunity to present my results on the EXA'05 conference. This work has been partially supported by the Russian Foundation for Basic Research under the grant No. 05-02-16618.

References

[1] M. Iwasaki, S.N. Nakamura, K. Shigaki, Y. Shimizu, H. Tamura, T. Ishikawa, R.S. Hayano, E. Takada, E. Widmann, H. Outa, M. Aoki, P. Kitching, and T. Yamazaki, Phys. Rev. Lett. **67**, 1246 (1991).

[2] H.A. Torii, R.S. Hayano, M. Hori, T. Ishikawa, N. Morita, M. Kumakura, I. Sugai, T. Yamazaki, B. Ketzer, F.J. Hartmann, T. von Egidy, R. Pohl, C. Maierl, D. Horváth, J. Eades, and E. Widmann, Phys. Rev. A, **59**, 223 (1999).

[3] T. Yamazaki, N. Morita, R.S. Hayano E. Widmann, and J. Eades, Phys. Reports **366**, (2002) 183.

[4] G.T. Condo, Phys. Lett. **9**, 65 (1964).

[5] R.S. Hayano, this proceedings.

[6] V.N. Efimov, Phys. Lett. **33B**, 563 (1970); Sov. J. Nucl. Phys. **12**, 589 (1971).

[7] M.C. George, L.D. Lombardi, and E.A. Hessels, Phys. Rev. Lett. **87**, 173002 (2001).

[8] K. Pachucki and J. Sapirstein, J. Phys. B **35**, 1783 (2002).

[9] K.S.E. Eikema, W. Ubachs, W. Vassen, and W. Hogervorst, Phys. Rev. A **55**, 1866 (1997).

[10] V.I. Korobov and A. Yelkhovsky, Phys. Rev. Lett. **87**, 193003 (2001).

[11] M. Hori, J. Eades, R.S. Hayano, T. Ishikawa, J. Sakaguchi, E. Widmann, H. Yamaguchi, H.A. Torii, B. Juhász, D. Horváth, and T. Yamazaki, Phys. Rev. Lett. **87**, 093401 (2001).

[12] M.I. Eides, H. Grotch, and V.A. Shelyuto, Physics Reports **342**, 63 (2001).

[13] L. Hilico, N. Billy, B. Grémaud, and D. Delande, Eur. Phys. J. D **12**, 449 (2000).

[14] S. Schiller, C. Lämmerzahl, Phys. Rev. A **68**, 053406 (2003).

[15] W.E. Caswell and G.P. Lepage, Phys. Lett. B **167**, 437 (1986)

[16] V.I. Korobov, Phys. Rev. A **54**, 1749 (1996).

[17] V.I. Korobov, D. Bakalov, and H.J. Monkhorst, Phys. Rev. A, **59**, R919 (1999).

[18] Y.K. Ho, Phys. Rep. **99**, 1 (1983).

[19] J. Aguilar and J.M. Combes, Commun. Math. Phys. **22**, 269 (1971); E. Balslev and J.M. Combes, *ibid.* **22**, 280 (1971); B. Simon, *ibid.* **27**, 1 (1972).

[20] V.I. Korobov, Phys. Rev. A **67**, 062501 (2003).